Design, manufacture, and testing of an open-source benchmark composite hydrokinetic turbine blade

M. González-Montijo, R. Murray, R. Beach, P. Murdy, V. S. Neary, D. Kim, and M. Wosnik

Abstract— **In a trend towards clean energy alternatives, recent years have seen great strides in the marine energy space. This has resulted in a pressing need for the design, development, and validation of novel energy harvesting technologies such as hydrokinetic devices, which capture kinetic energy from waves, tides, and currents. However, these devices span numerous concepts and designs that often lack solid benchmark research that can be freely referenced. This work focuses on the design process of an open-source composite hydrokinetic turbine blade for a three-bladed marine turbine rotor assembly with a diameter of 2.5 m. The proposed blade consists of two structural composite skins that are bonded with an adhesive and filled with a foam core. This study will explore and contrast the efficiency and resolution of low-fidelity rapid design methodologies and comprehensive high-fidelity approaches for the blade design, modeling, and analysis efforts, a key objective in this research. Blade hydrodynamic loads were modeled and applied to finite-element blade models to study deformations and potential failure. Ongoing efforts will result in blade manufacture and structural testing at the National Renewable Energy Laboratory. In future work, multiple blades will be deployed at the Living Bridge site at the University of New Hampshire and will be compared to rigid aluminum blades of the same geometry, developed by Sandia National Laboratories. Ultimately, this research will lay foundational groundwork for researchers and manufacturers, establishing a baseline composite blade design that will serve as a benchmark in the development of future hydrokinetic turbine blades.**

Keywords— **Composite hydrokinetic turbine blade, finite element modeling, marine renewable energy, open-source blade design**

I. Introduction

With the increasing threat of climate change, the importance of transitioning to clean energy sources is becoming clearer, making the development of alternative energy technologies a pressing need. In response, there has been a growing interest in developing alternative energy technologies, and marine and tidal energy have emerged as promising clean energy sources that could help countries, cities, and communities transition to low-carbon economies. In 2019, the U.S. Department of Energy's Water Power Technologies Office launched the Powering the Blue Economy™ (PBE) initiative and produced an extensive report presenting opportunities to leverage ocean resources to achieve economic, social, and environmental goals [1]. One of the technologies highlighted by this report is marine hydrokinetic (MHK) devices, which include underwater turbines that capture kinetic energy from water-based sources, such as waves, tides, and currents, to generate electricity. In the past two decades, MHK turbines have grown in popularity and potential in the clean energy sector [2]. These devices have the advantage of drawing from decades of accumulated knowledge from wind turbine research and development (R&D) efforts given the similarities in both systems. However, while MHK turbines hold much promise, they are still in a developmental phase and require further R&D to address challenges related to durability, efficiency, reliability, and cost-effectiveness. Moreover, the PBE report points out that these devices have little deployment experience in deep water, establishing a need for reliable demonstrations in deepwater locations with minimal deployment preparation.

This work was authored in part by the National Renewable Energy Laboratory, operated by Alliance for Sustainable Energy, LLC, for the U.S. Department of Energy (DOE) under Contract No. DE-AC36-08GO28308. Funding provided by the U.S. Department of Energy Office of Energy Efficiency and Renewable Energy Water Power Technologies Office. The views expressed in the article do not necessarily represent the views of the DOE or the U.S. Government. The U.S. Government retains and the publisher, by accepting the article for publication, acknowledges that the U.S. Government retains a nonexclusive, paid-up, irrevocable, worldwide license to publish or reproduce the published form of this work, or allow others to do so, for U.S. Government purposes.

M. Gonzalez-Montijo is with the University of Washington, Seattle WA, USA (email: gonzam8@uw.edu)

R. Murray, R. Beach, and P. Murdy are with the National Renewable Energy Laboratory, 15013 Denver West Parkway, Golden, CO 80401, USA

V.S. Neary, D. Kim are with the Sandia National Laboratories, 1515 Eubank Blvd SE, Albuquerque, NM 87123

M. Wosnik is with the University of New Hampshire, Durham, NH, USA

Digital Object Identifier: https://doi.org/10.36688/ewtec-2023-418

For marine current energy to reach commercialization, it requires investment in MHK turbine designs that can survive harsh subsea operating conditions. Optimizing turbine design and operation is essential to enhance efficiency and performance before widespread commercialization can be achieved. To develop these optimal turbine designs, relevant reference blade designs are needed to compare with innovations, and large-scale structural and performance data are critical to validate models and design processes. For example, researchers are exploring bend-twist coupled blades [3, 4] and blades made using novel materials and 3D-printing, but without a reference composite blade design, the impact of these technologies will be difficult to quantify. Additionally, tidal energy developers use design tools to estimate the loads and structural response of turbine blades at scale, but these tools typically are not validated at the same scale as they are being used to model, which introduces significant risk to future deployments.

There are currently very few, if any, open-source composite blade designs with associated structural and performance data at a large scale. To date, researchers have characterized open-source blade designs at small scale (less than 1 m diameter) in flumes and towing tanks [5-10], and industry has deployed blades with proprietary composite layups and designs. Some of these have included strain data collection, but without an open-source blade design, these data cannot easily be used for model verification by others [11]. Additionally, manufacturing methods and materials used at a small scale are not easily translated to larger-scale devices, and the mechanics of the larger blades are likely to greatly differ.

II. Objectives

The objective of this work is to design, build, and characterize a fully open-source, larger-scale composite tidal turbine blade. The blade design was based on the USDOE MHKF1 hydrofoils (blades) and turbine rotor, which were designed to serve as open-source prototypes with high techno-economic performance compared to existing hydrokinetic turbine hydrofoils and rotors (low capital and operations and maintenance costs, high annual energy production) that can be commercialized and deployed in energetic river, tidal or ocean current sites at a rated inflow current speed of 2.0 m/s at full scale [12]. Although, this is a standard unducted, three-bladed axial flow rotor, the hydrofoils were designed for marine environments and incorporated several novel design features to reduce the likelihood of cavitation and erosion, to minimize bio-fouling inboard by improved foil lift characteristics, and to reduce the potential for noise generation mid- and outboard by introducing hydrofoils with anti-singing trailing edges [13].

The 2.5-m reference MHKF1 turbine is currently under development by Sandia National Laboratories (Sandia) and the University of New Hampshire (UNH) Center for Ocean Renewable Energy (CORE). While the Sandia project will focus on the development of metal blades, this work will instead leverage the same optimized 2D foil sections and full 3D blade geometry [14] to produce analogous composite blades. Both blade designs will then be tested at CORE and compared.

The proposed composite blade will serve as a baseline reference for future innovative blade designs and manufacturing processes, thus accelerating innovation in the marine energy industry. For example, researchers can build on this composite design to include bend-twist coupling or 3D-printed materials. The structural models and manufactured blades could also serve as a reference for implementing and validating other numerical processes, such as water absorption at a representative scale. The blade will be manufactured using low-cost methods and materials, such as thermoplastic composites, which have improved seawater performance over traditional materials.

III. Blade Design and Analysis

Several composite blade design methodologies have been discussed in previous studies. Notably, a damage mechanics approach was used for tidal blade design [15], and a PreComp and finite-element analysis (FEA) process was employed for blade design [16]. A study utilizing a 1 m blade (of a similar scale to the MHKF1 blade) was also conducted, which involved comparing FEA results to digital image correlation from blade structural testing [17, 18]. The project presented herein involves a comprehensive five-step process aimed at the design, manufacturing, and testing of an open-source composite blade. The methodology for each of these steps is clearly defined and will be pursued in a systematic manner. This paper, however, will predominantly encapsulate the work carried out in Step 1. It should be noted that Steps 2 and 3 are ongoing efforts and will be presented in person at the 2023 EWTEC conference. The final stages, namely Steps 4 and 5, will form the basis of future research efforts. The steps are defined as follows:

1. **Composite Layup Design:** Developed a 1-m-long open-source reference composite blade.
   a. Initiate the design with low-fidelity modeling methods, incorporating NuMAD [19] and a finite-element model (FEM) established in ANSYS. This helped establish an initial composite layup through quick model iterations. Extreme loads were determined per IEC 62600-2 standards for marine energy system design using an OpenFAST model [20] of the MHKF1 blade and were implemented in the FEA. The layup underwent several iterations until span-wise strains at all blade locations remained under a strain limit of 2500 ue (or a maximum of 3500 ue considering a safety factor of 1.4).
   b. Following the determination of a baseline composite layup, a more comprehensive FEM was

developed. A failure analysis, using the Tsai Wu composite failure criteria, was subsequently conducted to ensure the design's durability during deployment.

2. **Performance Modeling:** Executing medium-fidelity performance modeling, using structural blade model inputs and inflow conditions for the UNH test site (ongoing work):
   a. An OpenFAST model has been developed, integrating blade structural properties such as flapwise and edgewise stiffnesses, distributed mass, and natural frequencies from PreComp and NuMAD.
3. **Manufacture:** The manufacturing and instrumenting of the reference composite blade using cutting-edge materials and cost-effective manufacturing techniques are currently in progress.
   a. This step involves a continuous iteration between manufacturing and design until a layup satisfies the manufacturing limits and is devoid of skin clashes.
4. **Testing:** Future work will structurally test the reference blade and Sandia metal blades to establish baseline mechanical properties and validate structural design models with the aforementioned data.
   a. The structural results will be used to verify the composite FEM models. This process will iterate between composite design and structural results until the final blade design is realized.
5. **Deployment:** The final stage will be the deployment of composite reference blades at UNH on the modular turbine currently being developed by Sandia. This will help to characterize the in-sea performance under a variety of conditions. The modular design of the UNH turbine will be leveraged during in-water testing to ensure cost-effectiveness.

A. Design Parameters: geometry, materials, and limits

The blade's geometry, shown in Fig. 1, is defined by a series of 20 hydrofoil cross sections developed through a collaborative effort between Sandia, the University of California, Davis, and the Applied Research Laboratory at Penn State University. Their unique geometric properties are meant to optimize the blade's performance and efficiency [12]. With a span of 1.05 m (1050 mm), the blade, while technically considered to be full-scale, is relatively short compared to other MHK blade designs.

Fig. 1. MHKF1 Blade.

The design holds an aggressive and nonlinear spanwise twist that ranges from 48 degrees at the root to 3.6 degrees at the tip, as can be appreciated in Figs. 2 and 3. The blade's hydrofoil chords range from 210 mm at the root to 306 mm (157 mm from root) and ramps down to 56.5 mm at the tip. The blade's aerodynamic center is positioned at 25% of the chord from the leading edge (LE).

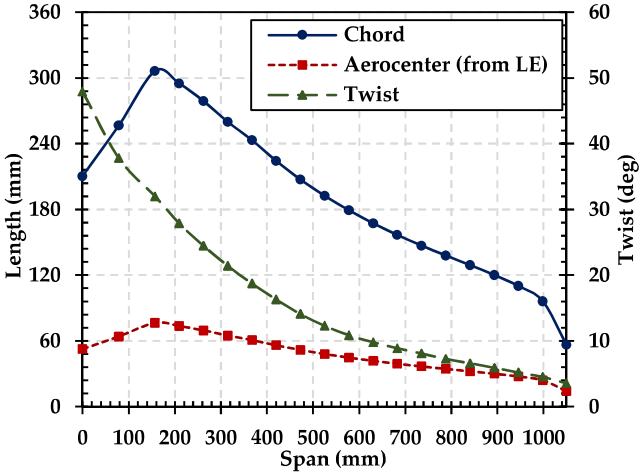

Fig. 2. Blade's spanwise chord, aerocenter, and twist.

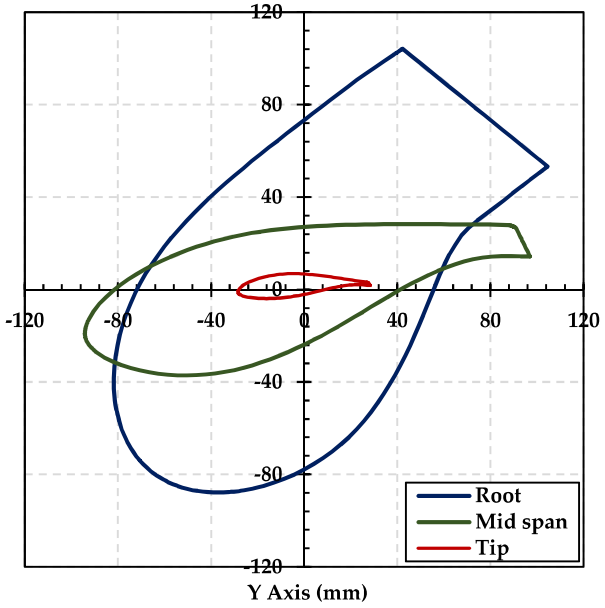

Fig. 3. Blade root, midspan, and tip cross sections as defined in AD model.

The overall blade design comprises several structural components that work together to withstand loads. The main component is the composite skin, which is made up of glass fiber composite material and allows for the blade's unique geometry. Additional unidirectional glass fiber strips, known as spar caps, span root to tip and serve as additional load-bearing components. A structural foam epoxy fills the inside of the blade shell to keep water out and achieve a close-to-neutral buoyancy. Other materials include a gelcoat to protect the blade from environmental elements, and the epoxy resin that is used to infuse the glass fiber layers, providing the blade with its strength and durability. Properties for these materials can be found in Table I.

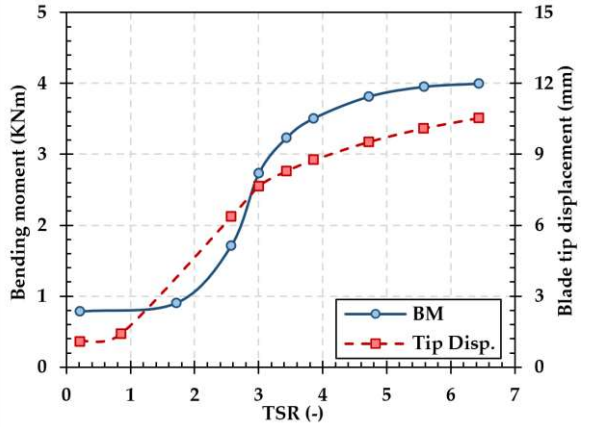

Fig. 4. Root bending moment and tip displacement as a function of TSR from OpenFAST. The loads at the design TSR of 5.6 were used for the initial FEM development.

Once blade components were defined and materials selected, design limits were established by adhering to industry standards prevalent in the wind turbine sector. The primary goal was to ensure structural integrity and enhance blade performance. The blade layup was guided by a conservative approach, which entailed setting a global blade strain limit of 3500 microstrain and a maximum deflection limit of 10% blade span (105 mm). With the inclusion of a safety factor of 1.75, this translated to an overall effective limit of 2000 microstrain (the deflection limit was retained). However, certain sections of the blade, where the modeling fidelity was comparatively lower, were permitted to exceed this 2000 microstrain limit. In anticipating potential composite failure, Tsai Wu's criteria were also adopted as the primary failure criteria.

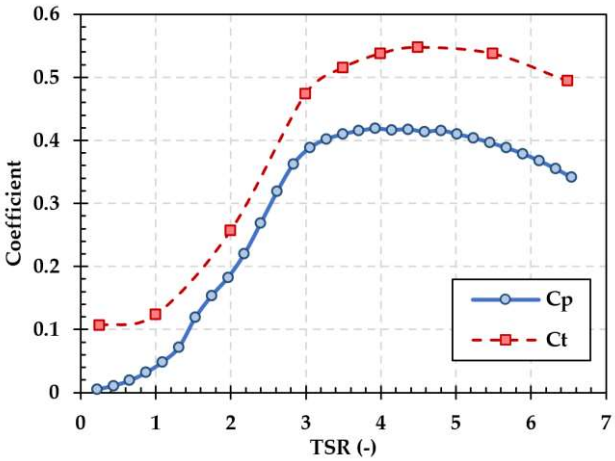

Fig. 5. Power (Cp) and thrust (Ct) coefficients as a function of tip speed ratio for the rotor.

B. *Loading conditions: low- and high-fidelity modeling*

Understanding the blade's operational environment is crucial, as it demands the simultaneous consideration of both flow and rotational speeds to accurately represent loading conditions. These conditions subsequently shape the design and robustness of the composite layup. In this regard, OpenFAST, a multi-physics, multi-fidelity open-source wind turbine simulation tool [20], was employed to develop a turbine model; leveraging the AeroDyn and ElastoDyn modules to determine the blade root bending moments for the initial low-fidelity design. A design flow speed of 3 m/s coupled with a rotational speed of 130 rpm were set as conservative operation parameters. The OpenFAST model yielded blade loads, displacements, and power and thrust coefficients across a comprehensive range of tip speed ratios (TSR), as depicted in Figs. 4 and 5, respectively. Fig. 4 portrays the blade deflection as a function of the tip speed ratio, as simulated through the OpenFAST framework. A maximum deflection of approximately 10.5 mm was recorded, which when compared to results yielded by a subsequent blade FEM, as discussed later in this paper, seemed to slightly underestimate the deformations. This discrepancy can be ascribed to the use of lower-resolution structural inputs and unique simulation environment inherent to the ElastoDyn module of OpenFAST.

Emergency shutdown scenarios were also tested in OpenFAST to confirm that the loads under these conditions would not surpass those utilized in the blade design, all under steady flow conditions. A simplified static three-point load scenario was also established from these loads, which resulted in a bending moment diagram nearly identical to

TABLE I. MATERIAL PROPERTIES

		Ex	Ey	Gxy	prxy	
	Ply Thickness	E11	E22	G12	v12	Density
Material	[mm]	[GPa]	[GPa]	[GPa]	[-]	[kg/m^3]
Seartex UD	0.737	42	12	3.7	0.27	1182
Seartex Biax	0.475	11.94	11.94	12.13	0.27	614

the original (see Fig. 6) and is intended for use in a low-fidelity model, which will be discussed further in the next section.

Following this, a computational fluid dynamics (CFD) model was constructed to attain a pressure distribution over the blade under the same design conditions. This model provided a more precise load application method for the FEMs. It also served to corroborate the bending moments determined through OpenFAST, with a strong congruity observed in results, as also evidenced in Fig. 6.

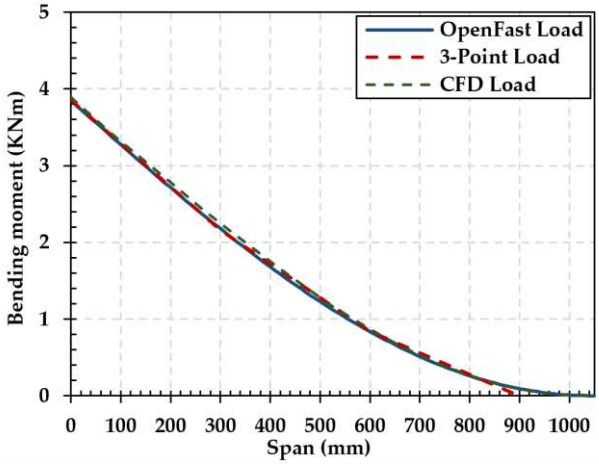

Fig. 6. Bending moment diagrams.

Future efforts in this space include incorporating turbulence using TurbSim, along with added mass and buoyancy effects in the OpenFAST model. These features are currently under development for the OpenFAST package.

C. *Low-fidelity modeling and preliminary design iteration*

In the context of turbine blade design, where rapid design iteration is crucial for efficiency, a preliminary low-fidelity design approach that leverages the capabilities of the open-source software tool NuMAD 3.0 (Numerical Manufacturing and Design) is often employed. This intuitive platform is particularly adept at streamlining the creation of three-dimensional blade models, managing all pertinent blade information from aerodynamic to material properties, and enabling both manual and auto-optimization of the blade data [19].

NuMAD's user-friendly interface facilitates this process by allowing us to readily input a layup schedule via an Excel spreadsheet. These data are then used to generate a shell FEM in a cantilever configuration (fixed at the root) through a MATLAB-based graphical user interface (see Fig. 7). ANSYS APDL was then used to quickly processes the FEM, applying the aforementioned three-point load case via simple APDL scripting.

This approach produced blade deflection and normal elastic strain results for each iteration within a 10–15-minute time frame. Such rapid cycling between design and analysis enables comprehensive exploration of the design space, leading to swift identification and refinement of promising layup configurations. Consequently, this method greatly enhanced the efficiency of the design process and reduced

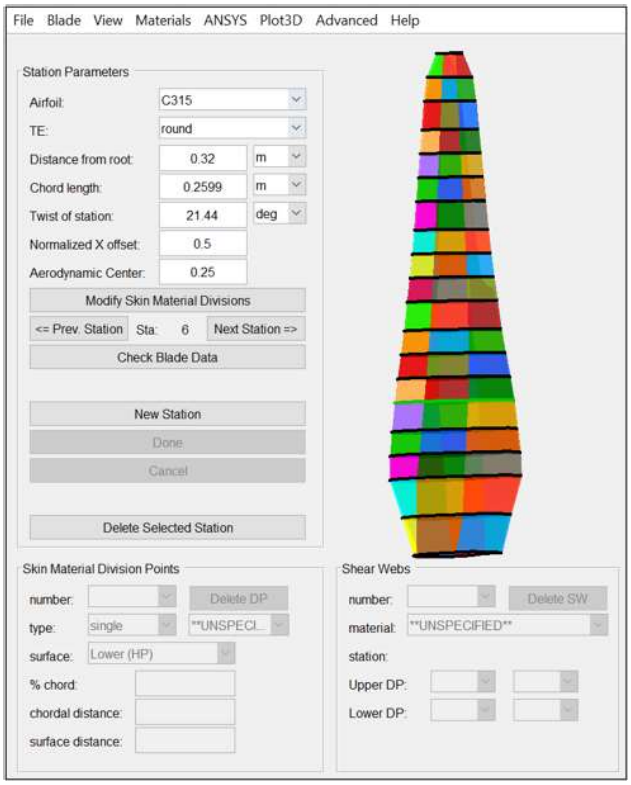

Fig. 7. NuMAD graphical user interface and NuMAD generated model.

computational resource demands, establishing a robust preliminary blade design with far less time investment.

Through this process, the geometric properties of the spar caps were determined as well. For manufacturing simplicity, the spar caps were positioned at the 50% chord. Although potential misalignment moments from the aerodynamic center were assessed, they were not deemed a critical concern. The spar caps were determined to be 120 mm wide and 13.3 mm thick at the root, which would taper down across the span to 25 mm wide and 0.737 mm thick at the tip. This configuration ensures a large enough surface area at the root for creating a secure attachment mechanism between the composite skins and the hub. This design allows the spar caps to bear most of the blade's loads, while the composite skins contribute additional stiffness and fulfill the necessary aerodynamic requirements.

D. *High-fidelity modeling and final design calibration*

In the pursuit of a robust and dependable design, a comprehensive examination of the blade's complex geometric features and their impact on strain distributions is of utmost importance. This level of scrutiny demanded the use of a high-fidelity FEM, which was developed using the Ansys Workbench (AWB) platform and the Ansys Composite PrepPost (ACP) tool (see Fig. 8). This detailed analytical process proved highly valuable for detecting potential design weaknesses in both the high- (HP) and low-pressure (LP) surfaces as well as in lower-resolution areas (i.e., trailing edge (TE) and LE areas near the tip) and offers great potential for automation once the user is adept.

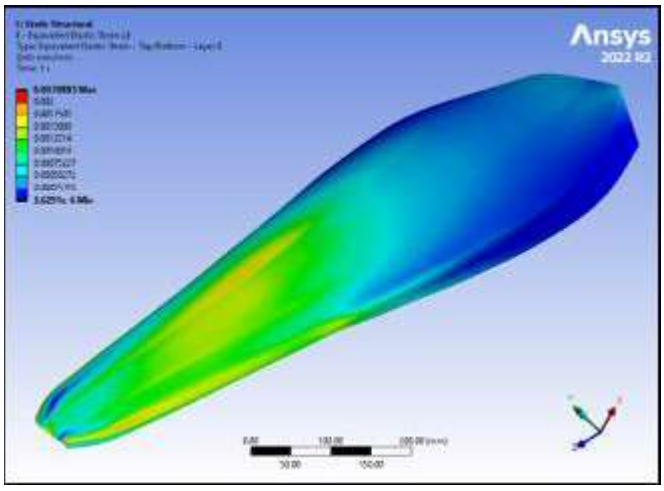

Fig. 8. Ansys AWB – equivalent elastic strains.

The MHKF1 blade design incorporates unconventional features, such as unique TE definitions that transition from a thick, flat surface to a thin, sharp edge, with twist and tapering along the span. To accommodate this level of complexity, the versatile capabilities of AWB were harnessed. Notably, AWB allowed for the direct application of detailed CFD loads to the model, superseding the simplified three-point load case used in the low-fidelity model and enhancing the accuracy of the loading condition representation. The CFD model used to obtain said loads was developed by importing the AWB generated mesh into Simcenter STAR-CCM+, a CFD based simulation software, and using the same parameters employed for the OpenFAST simulation.

In parallel, ACP provided the framework for defining the blade's comprehensive composite layup scheme. This tool enabled precise stagger ply drops in the FEM, a crucial feature for avoiding sharp changes in composite stiffness along the span, which had been observed to lead to significant localized strain concentrations in the previous low-fidelity approach.

E. Results: Comparison of low-and high-fidelity FEMs

Low- and high-fidelity design approaches were compared with a twofold aim: validating the model outcomes and determining the proximity of the low-fidelity approach to a high-level solution. The final iteration of the composite layup design obtained through the low-fidelity method is presented in Table II (where SCs = spar caps, BX = Biaxial plies, UD = Unidirectional plies, LF = low-fidelity, and HF = high-fidelity). This layout defines the number of plies of each material at each of the hydrofoil stations initially used to define the blade geometry. Concurrently, Table II also includes the composite layup design achieved through the high-fidelity approach, exhibiting minor deviations from the low-fidelity design due to the precise ply cutoff distance definitions enabled by AWB. Deflections and strains were analyzed for both approaches. Fig. 9 illustrates deformations for the low- and high-fidelity models, exhibiting maximum tip deflections of 15 mm and 14 mm, respectively, alongside the spanwise twist of the

TABLE II. COMPOSITE LAYUP DESIGN: NUMBER OF PLIES ACROSS SPAN

Span (mm)	SCs		BX		UD	
	LF	HF	LF	HF	LF	HF
0	18	18	18	18	18	18
78.66	18	18	18	18	18	18
157.3	16	18	16	18	16	17
209.9	14	17	14	16	14	16
262.5	12	15	12	14	12	14
315.1	10	13	10	13	10	12
367.6	9	12	9	11	9	10
420.2	8	10	8	9	8	9
472.8	7	8	7	7	7	7
525.4	6	7	6	6	6	6
577.9	6	7	6	6	6	6
630.5	6	7	6	6	6	6
683.1	6	7	6	6	6	6
735.7	6	7	6	6	6	6
788.3	6	7	6	6	6	6
840.8	5	7	5	6	5	5
893.4	4	6	4	5	4	4
946	3	4	3	4	3	3
998.6	2	2	2	3	2	2
1050	1	1	2	2	2	2

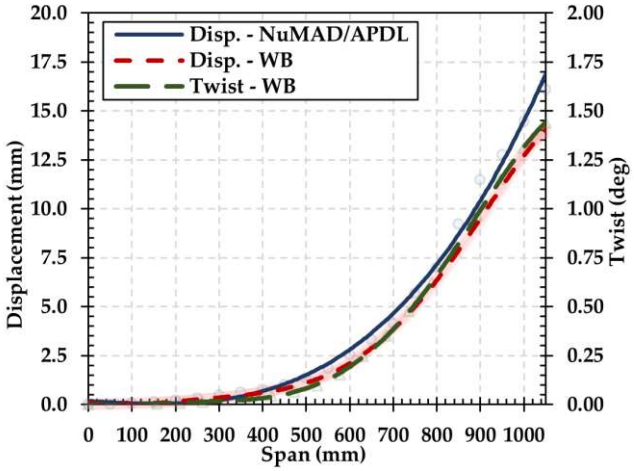

Fig. 9. Blade deformations: tip displacement and twist

blade as per AWB. Further, Fig. 10 juxtaposes the normal elastic strains for both cases, including the low-fidelity model's maximum case (Y) and a more comprehensive look at all directions in the high-fidelity model. This comparison not only delineates maximum strain values at the spar cap locations where most of the load is concentrated but also highlights the variations in normal strains between the simplified three-point load scenario and the direct application of CFD loads.

This observation revealed higher transverse strains for the three-point load case and dominating longitudinal strains for the CFD loads. This disparity can be attributed to the complexity of CFD pressures, encompassing significant centrifugal and transverse forces that impact the entire strain nexus across the composite skin, an aspect absent in the three-point load scenario. Utilizing the flexibility of AWB, normal strains for the LE and TE were also obtained

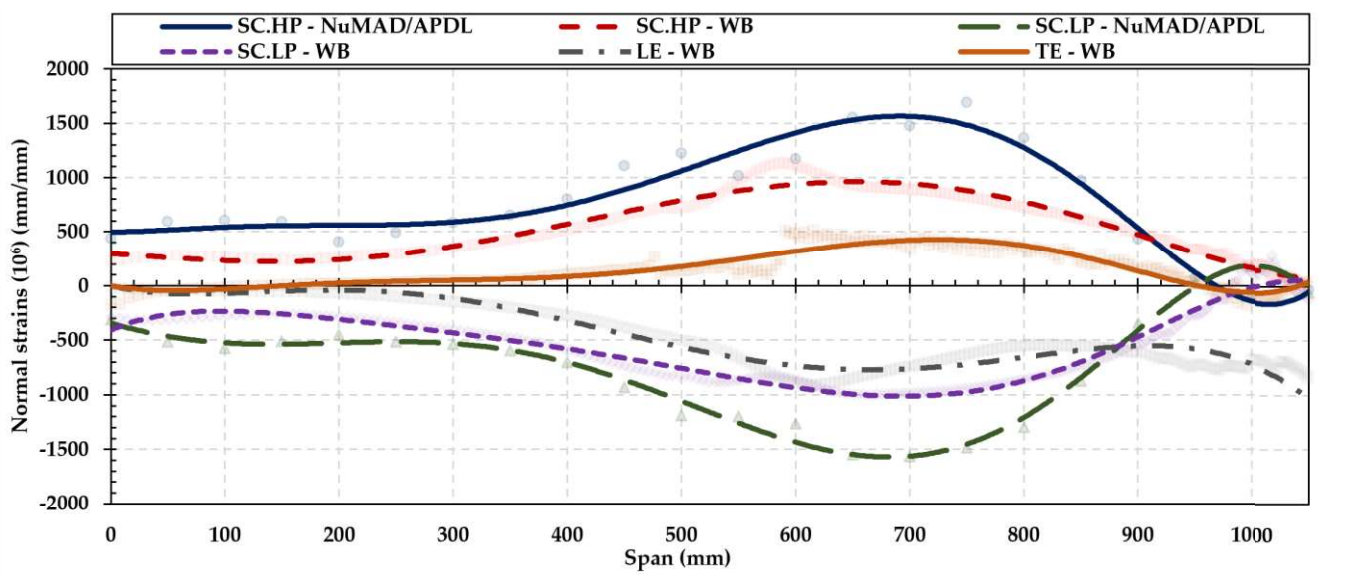

Fig. 10. Maximum normal elastic strains.

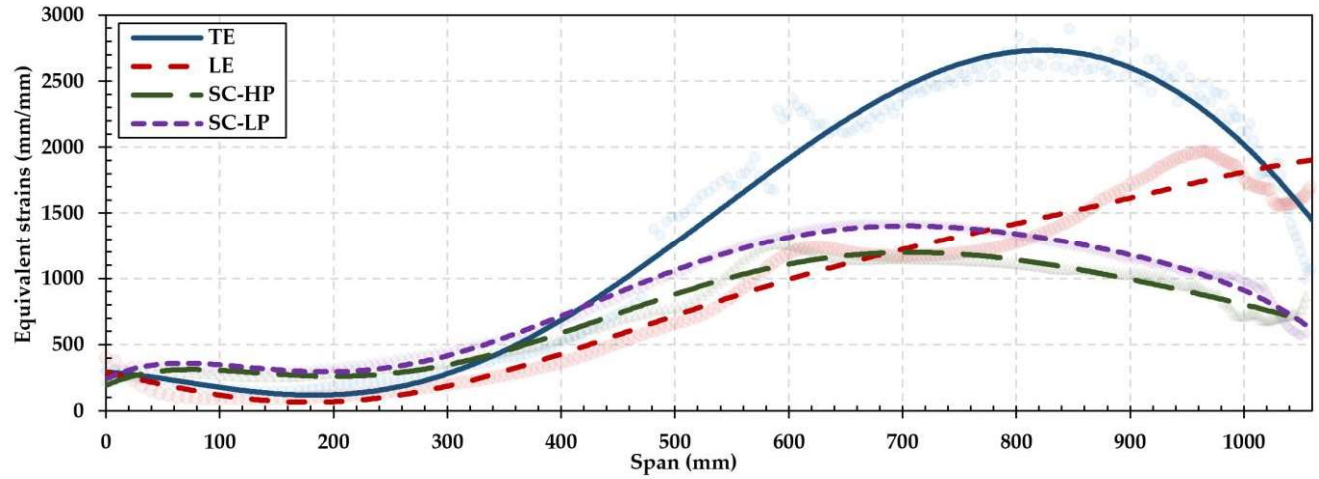

Fig. 11. Maximum equivalent elastic strains.

and incorporated in Fig. 10. Importantly, neither deflections nor normal strains were observed to surpass the predetermined limits of 105 mm and 2000 microstrain.

Abiding by common industry practices, equivalent (Von-Mises) strains (EQVs) were also analyzed (see Fig. 11), a method often employed in the wind industry as a conservative measure to inform composite blade design. Although EQVs are less representative of the actual strain state, they offer a more streamlined method of analysis and can reveal potential weaknesses overlooked in normal strains. In this case, EQVs identified potential inaccuracies in modeling the TE and LE near the blade tip. To mitigate these inconsistencies, a 25.4-mm epoxy bond line was added inside the TE using solid elements, simulating the real-world epoxy bonding in the blade region. This addition brought uniformity to the TE deformations, but EQVs at the TE were still found to exceed the 2000 microstrain limit, suggesting a need for special consideration for this area during blade testing or deployment. Final blade specifications, including the number of plies per component, composite thickness, and ply cutoff locations, are presented in Figs. 12 and 13.

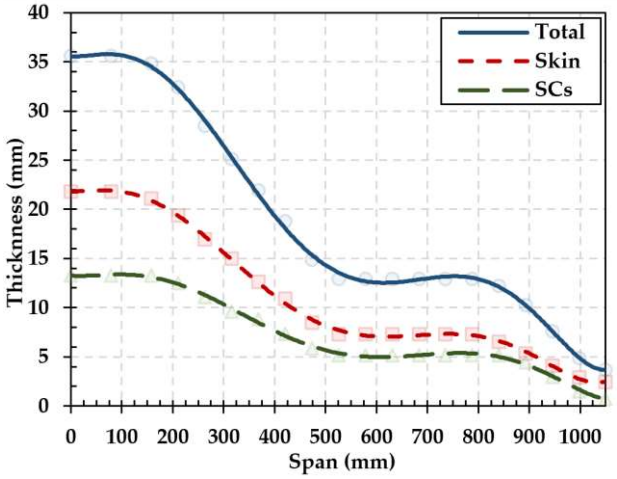

Fig. 12. Final design layers and spanwise thickness.

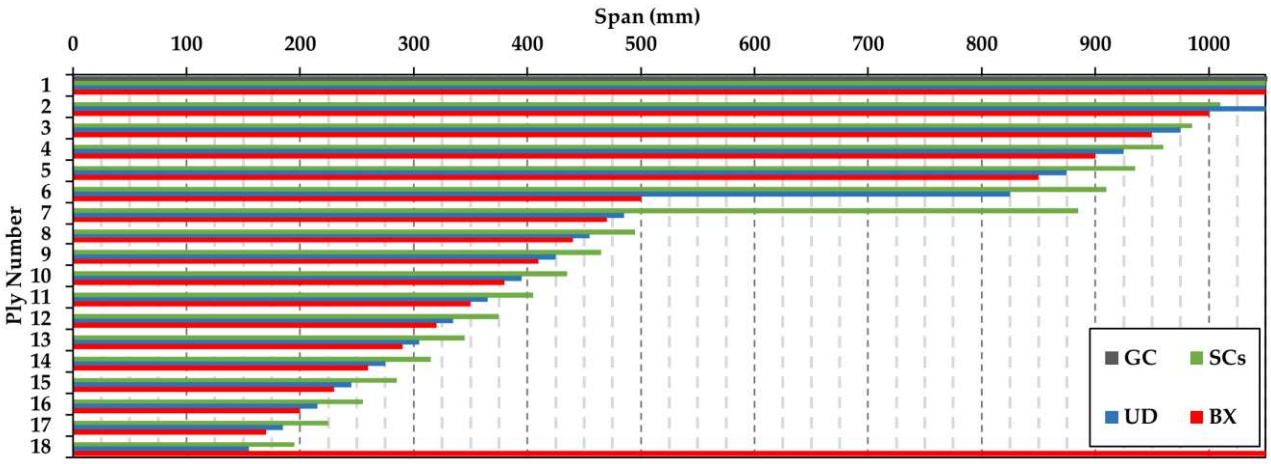

Fig. 13. Ply cutoffs.

A failure analysis was also carried out in ACP using Tsai Wu's failure criteria, which predicts failure at a value of 1 [21-22]. The results registered a maximum value of 0.2, as depicted in Fig. 14, which suggests a safety factor of 5 for failure in this method.

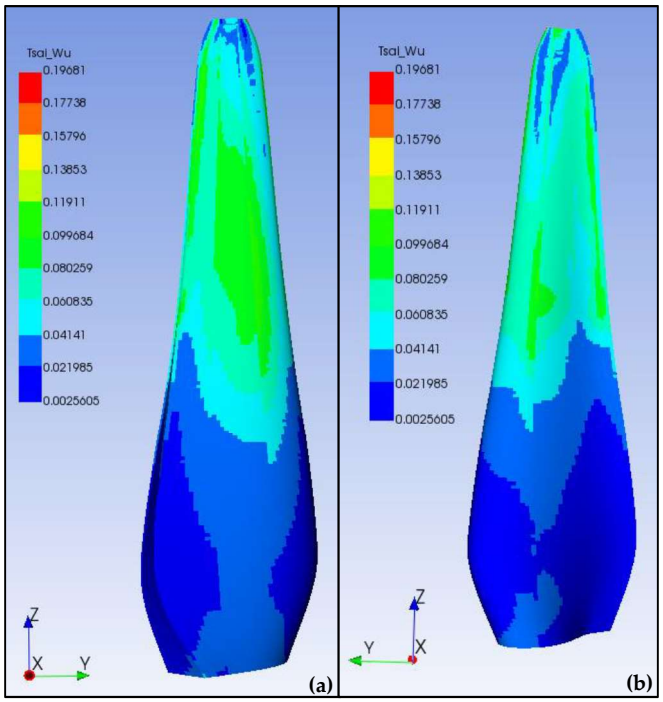

Fig. 14. Failure analysis using Tsai Wu: LP (a) and HP (b) surfaces.

IV. MANUFACTURING

Upon finalizing the composite layup design and determining ply cutoff points, precise CAD cut-files were produced to guide an Eastman composite cutter machine in cutting the plies from material rolls. These cut plies were meticulously arranged in CNC-machined aluminum molds that replicated the external surface geometries of the blade. Subsequently, these laid-out plies were bagged, infused with a thermoset resin, and allowed to cure. Post curing, the blades were carefully demolded, and their dimensions were verified.

This initial production was essentially an exploratory "first-pass," intended to identify and evaluate any manufacturing complexities or defects that might emerge. It was discerned that an additional 50 mm ply length should be included at the root of all plies to maintain uniformity as the plies accumulate. Additionally, it was found necessary to taper the plies horizontally to prevent skin clashing near the LE and TE. Furthermore, dry patches were noticed on the mold side of the skins, as can be discerned in Fig. 15. This issue is likely due to the nature of the ply build up in the patch area, which makes resin flow more difficult. This will be addressed in future skin manufacturing by adjusting the flow media layout and extending infusion time to foster resin flow to the area.

This iterative and practical manufacturing process, aimed at refining the final blade design, was conducted at the Composites Manufacturing Education and Technology Facility at the National Renewable Energy Laboratory (NREL).

Fig. 15. Composite blade skins.

V. CONCLUSIONS AND CONTINUED RESEARCH

A baseline composite MHK blade was designed, modeled, and analyzed using advanced simulation methodologies of different fidelities. Partial manufacturing of the blade's HP and LP skins was achieved, which informed final design decisions and will help refine the manufacturing process going forward.

Both low- and high-fidelity modeling approaches and tools were employed, providing results at different

resolution levels. This process outlined a quick method for determining an initial composite blade design, and a subsequent, more reliable, yet resource-heavy, process that corroborated initial results.

Normal strains were maintained below a threshold of 2000 microstrain, while EQVs were used as a tool to identify potential areas of concern, primarily around the TE and LE near the blade tip. Blade deflection was also monitored and maintained well within safe levels.

Once completely manufactured, the fully assembled blade is scheduled to undergo comprehensive testing, including both static and fatigue examinations. The blade is projected to be deployed at the UNH CORE facility where it will be compared with analogous aluminum blades of identical geometry to determine their performance.
Finally, this research marks a vital stride toward advancing PBE initiatives and harnessing MRE resources for a clean energy future. The benchmark design established by this project will hold significant implications for more efficient and durable MRE infrastructure, advancing sustainable energy solutions to help address climate change.

ACKNOWLEDGEMENTS

The authors would like to extend their gratitude to Dr. Thanh Toan Tran, for his contribution on the employed CFD analysis, which provided the necessary modeling loads.

The authors are also grateful to Dr. Pietro Bortolotti and Dr. Mayank Chetan, from NREL, and Alejandra Escalera Mendoza and Professor Todd Griffith, from The University of Texas at Dallas, for their support, feedback, and input throughout the blade design and modeling processes.

REFERENCES

[1] LiVecchi, A., A. Copping, D. Jenne, A. Gorton, R. Preus, G. Gill, H. R. Green, S. Geerlofs, S. Gore, D. Hume, W. McShane, C. Schmaus, and Spence, "Powering the Blue Economy; Exploring Opportunities for Marine Renewable Energy in Maritime Markets.," Washington, D.C., 2019.

[2] M. P. Mike J. Beam, Brian L. Kline, Brian E. Elbing, William Straka, Arnold A. Fontaine, Michael Lawson, Ye Li, Robert Thresher, "Marine Hydrokinetic Turbine Power-Take-Off Design for Optimal Performance and Low Impact on Cost-of-Energy," in ASME 2013 32nd International Conference on Ocean, Offshore and Arctic Engineering, 2013, pp. 1–9.

[3] R. Murray, "Passively adaptive tidal turbine blades: Design tool development and initial verification," Dalhousie University, 2016.

[4] K. E. Porter *et al.*, "Flume testing of passively adaptive composite tidal turbine blades under combined wave and current loading," *J. Fluids Struct.*, vol. 93, p. 102825, 2020.

[5] D. A. Doman, R. E. Murray, M. J. Pegg, K. Gracie, C. M. Johnstone, and T. Nevalainen, "Tow-tank testing of a 1/20th scale horizontal axis tidal turbine with uncertainty analysis," *Int. J. Mar. Energy*, vol. 11, pp. 105–119, 2015.

[6] L. Myers and A. S. Bahaj, "Power output performance characteristics of a horizontal axis marine current turbine," *Renew. Energy*, vol. 31, no. 2, pp. 197–208, 2006.

[7] A. F. Molland, A. S. Bahaj, J. R. Chaplin, and W. M. J. Batten, "Measurements and predictions of forces, pressures and cavitation on 2-D sections suitable for marine current turbines," *Proc. Inst. Mech. Eng. Part M J. Eng. Marit. Environ.*, vol. 218, no. 2, pp. 127–138, Jun. 2004.

[8] P. W. Galloway, L. E. Myers, and A. S. Bahaj, "Experimental and numerical results of rotor power and thrust of a tidal turbine operating at yaw and in waves," in *Proceedings of the World Renewable Energy Congress*, 2011, pp. 2246–2253.

[9] W. M. J. Batten, A. S. Bahaj, A. F. Molland, and J. R. Chaplin, "Hydrodynamics of marine current turbines," *Renew. Energy*, vol. 31, no. 2, pp. 249–256, 2006.

[10] W. M. J. Batten, A. S. Bahaj, A. F. Molland, and J. R. Chaplin, "Experimentally validated numerical method for the hydrodynamic design of horizontal axis tidal turbines," *Ocean Eng.*, vol. 34, no. 7, pp. 1013–1020, 2007.

[11] T. Lake *et al.*, "Strain gauge measurements on a full scale tidal turbine blade," *Renew. Energy*, vol. 170, pp. 985–996, 2021.

[12] A. A. Fontaine, W. A. Straka, R. S. Meyer, M. L. Jonson, S. D. Young, and V. S. Neary, "Performance and wake flow characterization of a 1:8.7-scale reference USDOE MHKF1 hydrokinetic turbine to establish a verification and validation test database," *Renew. Energy*, vol. 159, pp. 451–467, 2020.

[13] H. Shiu et al., "A Design of a Hydrofoil Family for Current-Driven Marine-Hydrokinetic Turbines." pp. 839–847, 30-Jul-2012.

[14] V. S. Neary et al., "Marine Hydrokinetic Axial Flow Rotor Assembly," United States Patent Appl. 63/284,742, 2022.

[15] E. M. Fagan, C. R. Kennedy, S. B. Leen, and J. Goggins, "Damage mechanics based design methodology for tidal current turbine composite blades," *Renew. Energy*, vol. 97, pp. 358–372, 2016.

[16] D. M. Grogan, S. B. Leen, C. R. Kennedy, and C. M. Ó Brádaigh, "Design of composite tidal turbine blades," *Renew. Energy*, vol. 57, pp. 151–162, 2013.

[17] H. Gonabadi, A. Oila, A. Yadav, and S. Bull, "Fatigue life prediction of composite tidal turbine blades," *Ocean Eng.*, vol. 260, p. 111903, 2022.

[18] H. Gonabadi, A. Oila, A. Yadav, and S. Bull, "Structural performance of composite tidal turbine blades," *Compos. Struct.*, vol. 278, p. 114679, 2021.

[19] J. Berg and B. Resor, "Numerical manufacturing and design tool (NuMAD V2. 0) for wind turbine blades: User's guide," *Sandia Natl. Lab. Albuquerque, NM, Tech. Rep. No. SAND2012-728*, no. August, pp. SAND2012-7028, 1051715, 2012.

[20] "OpenFAST | Wind Research", [online] Available: https://www.nrel.gov/wind/nwtc/openfast.html.

[21] M. Leong, L. C. T. Overgaard, I. M. Daniel, E. Lund, and O. T. Thomsen, "Interlaminar/interfiber failure of unidirectional glass fiber reinforced composites used for wind turbine blades," J. Compos. Mater., vol. 47, no. 3, pp. 353–368, 2013.

[22] M. Ozyildiz, C. Muyan, and D. Coker, "Strength Analysis of a Composite Turbine Blade Using Puck Failure Criteria," J. Phys. Conf. Ser., vol. 1037, no. 4, 2018.